High-J_c MgB_2 Josephson junctions with operating temperature up to 40 K

Ke Chen,[1,a),b)] C. G. Zhuang,[1,b)] Qi Li,[1] Y. Zhu,[2] P. M. Voyles,[2] X. Weng,[3] J. M. Redwing,[3] R. K. Singh,[4] A. W. Kleinsasser,[5] and X. X. Xi[1,3,b)]
[1]*Department of Physics, The Pennsylvania State University, University Park, Pennsylvania 16802, USA*
[2]*Department of Materials Science and Engineering, University of Wisconsin, Madison, Wisconsin 53706, USA*
[3]*Department of Materials Science and Engineering, The Pennsylvania State University, University Park, Pennsylvania 16802, USA*
[4]*School of Mechanical, Aerospace, Chemical and Materials Engineering, Arizona State University, Tempe, Arizona 85287, USA*
[5]*Jet Propulsion Laboratory, Pasadena, California 91109, USA*

(Received 1 December 2009; accepted 29 December 2009; published online 28 January 2010)

Sandwich-type $MgB_2/MgO/MgB_2$ Josephson junctions with Au or MgB_2 interconnection were fabricated using hybrid physical-chemical vapor deposited MgB_2 thin films and RF-magnetron-sputtered MgO barrier. The junctions show properties similar to those in high-J_c Nb junctions with J_c up to 275 kA/cm^2 at 4 K, which remains nonzero up to 40 K. Critical current modulations by applied magnetic field and constant voltage steps under microwave radiation were observed. Combined with the larger energy gaps in MgB_2 than in Nb, the junctions presented here allow simple MgB_2 digital circuits to work over 20 K or with a clock speed above 1 THz. © *2010 American Institute of Physics*. [doi:10.1063/1.3298366]

Superconducting integrated circuits using Josephson junctions have higher speed and lower power consumption than semiconductor circuits.[1–3] However, the only mature technology uses Nb (critical temperature T_c=9.25 K), which requires a low operating temperature of about 4 K. Superconducting circuits using the 40 K superconductor MgB_2 can operate above 20 K (Ref. 4) cooled by more efficient, more compact, and less costly cryocoolers than those used at 4 K.[5] Such a breakthrough requires fabrication technologies for MgB_2 Josephson junctions with high critical current density J_c and multilayers consisting of superconducting, insulating and resistive films. There have been reports of Josephson junctions with one MgB_2 and one low-T_c superconductor electrodes,[6–8] which cannot operate above the lower T_c. All-MgB_2 weak-link junctions[9–13] are not ideal for integrated circuits. All-MgB_2 sandwich-type Josephson junctions have been reported,[14–16] some with near-ideal Fraunhofer patterns, however, the J_c values are very low and drop quickly to zero at 20–25 K. In this letter, we report $MgB_2/MgO/MgB_2$ sandwich-type Josephson junctions with high J_c up to 275 kA/cm^2 at 4 K, which remains nonzero up to 40 K.

The ultimate speed limit of Josephson junction-based rapid single flux quantum (RSFQ) circuits is proportional to the product I_cR_n, where I_c is the critical current and R_n the resistance of the junction in the normal state.[1] To eliminate hysteresis in $I-V$ characteristics, tunnel junctions in RSFQ circuits are usually critically damped by an external shunt resistor, and the maximum circuit speed is approximately proportional to $J_c^{1/2}$.[17] The highest operating speed for Nb circuit, 770 GHz, has been demonstrated by an RSFQ toggle flip-flop (TFF) frequency divider with J_c greater than 60 kA/cm^2.[18] The energy gap in MgB_2 (~2.2 meV for the smaller of the two gaps[19]) is larger than that of Nb (~1.5 meV), implying a limiting clock speed for MgB_2 digital circuits of above 1 THz.[2,18]

The structure of the $MgB_2/MgO/MgB_2$ sandwich-type Josephson junctions were illustrated in Fig. 1(a). A 100 nm-thick MgB_2 film was first grown on a SiC(0001) substrate by hybrid physical-chemical vapor deposition (HPCVD)[20] at 710 °C under conditions similar to those described in Ref. 8. The root-mean-square roughness of the MgB_2 film was 1.2–1.5 nm. The sample was then transferred in air to an rf magnetron sputtering system, where a 0.8–2 nm-thick MgO film was deposited at room temperature from a 2 inch MgO ceramic target at 25 W (130V) in 0.4 Pa pure Ar. The deposition rate was approximately 0.024 nm/min. The sample was

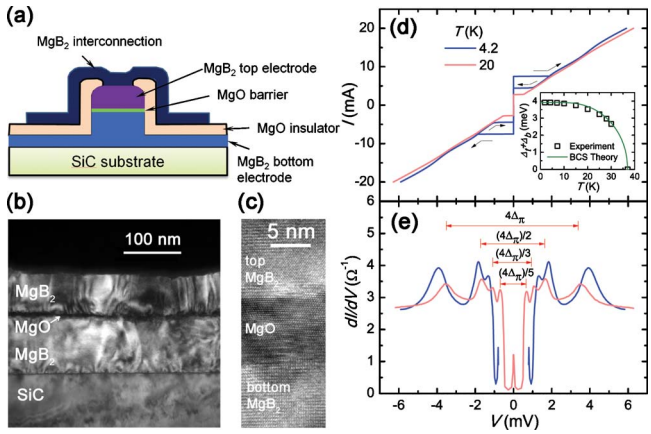

FIG. 1. (Color online) (a) Illustration of the junction structure. (b) Low magnification and (c) high resolution TEM cross-sectional view of the trilayer structure. The epitaxial relationship is $MgB_2[0001]\|MgO[111]\|MgB_2[0001]\|SiC[0001]$ and $MgB_2[1\bar{1}00]\|\times MgO[1\bar{2}1]\|MgB_2[1\bar{1}00]\|SiC[1\bar{1}00]$. (d) $I-V$ and (e) $dI/dV-V$ characteristics of a junction at 4.2 and 20 K. The arrows indicate the direction of current sweep at 4.2 K. (inset) The temperature dependence of the sum of energy gaps of both electrodes (symbols) compared to the Bardeen-Cooper-Schrieffer theory (line). Subgap peak positions for 20 K are indicated.

a)Electronic mail: kchen@temple.edu.
b)Present address: Department of Physics, Temple University, Philadelphia, Pennsylvania 19122, USA.

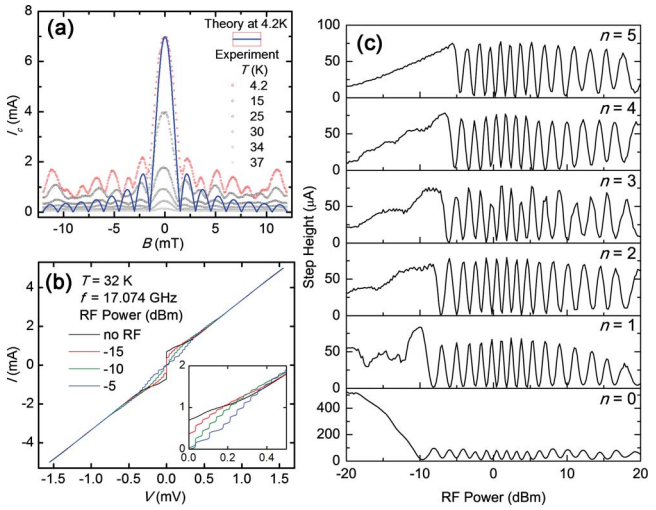

FIG. 2. (Color online) (a) I_c modulation by applied magnetic field at temperatures from 4.2 to 37 K (symbols) compared to the and theoretical Fraunhofer pattern (line) and (b) $I-V$ curves under 17.047 GHz microwave radiation for a 20×20 μm^2 junction. (c) The microwave power dependence of the Shapiro steps for n from 0 to 5.

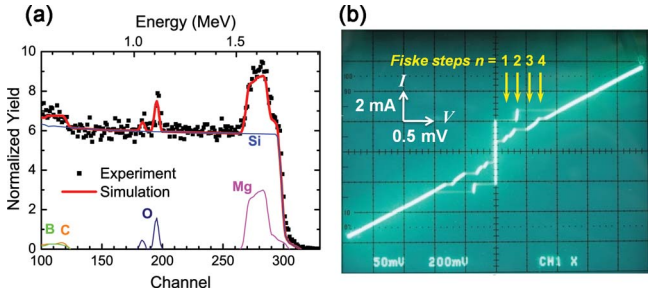

FIG. 3. (Color online) Measurement of the MgO barrier thickness by (a) RBS spectrum (squares, 3.05 MeV, He^{2+}) and simulation (thick line) of an $MgB_2/MgO/MgB_2$ trilayer, suggesting a well defined 1.6-nm-thick MgO layer sandwiched between the MgB_2 electrodes, and by (b) the Fiske steps indicated by arrows on the $I-V$ curve of a 70×70 μm^2 junction under 0.1 mT field at 4.2 K with the MgO barrier thickness calculated to be about 1.2 nm.

then transferred back to the HPCVD reactor for deposition of a 67 nm-thick top MgB_2 electrode. Square-shaped junctions with sizes from 4×4 to 70×70 μm^2 were defined by photolithography and ion milling. After a subsequent sputter deposition of a 100 nm-thick MgO insulating layer and lift-off, an interconnection layer of gold or HPCVD MgB_2 film was deposited. For genuine four-probe measurement, the contact to the top electrode was separated into two parts in the case of gold interconnection. Transmission electron microscope (TEM) cross-section images of a $MgB_2/MgO/MgB_2$ trilayer are shown in Figs. 1(b) and 1(c). All layers are epitaxial with each other and with the SiC(0001) substrate. Both MgB_2/MgO interfaces are sharp without indication of interdiffusion.

The $I-V$ characteristics of a $MgB_2/MgO/MgB_2$ junction at 4.2 and 20 K are shown in Fig. 1(d). Hysteresis is pronounced at 4.2 K, becoming smaller as temperature increases, and eventually disappearing at around 20 K. The behavior can be accounted for by the resistively shunted junction model.[1] Figure 1(e) shows the $dI/dV-V$ curves for the two temperatures. Two energy gaps exist in MgB_2, arising from the quasi-two-dimensional and *ab*-plane-confined σ bands $[\Delta_\sigma(0)=7.4$ meV] and the three-dimensional π bands $[\Delta_\pi(0)=2.2$ meV].[21,22] The two dI/dV peaks at around ±4 mV correspond to the sum of the π gaps of the top and bottom MgB_2 electrodes. Subgap peaks roughly at $2\Delta_\pi/N$ ($N=2$, 3, and 5) are due to multiple Andreev reflection (MAR).[23] There is no observation of the σ gap because less than 1% of σ-band current is expected in *c*-axis tunneling.[24]

Figure 2(a) shows I_c of a $MgB_2/MgO/MgB_2$ junction versus magnetic field B applied in the junction plane at temperatures from 4.2 to 37 K. A periodic modulation resembling the expected Fraunhofer pattern is observed. From the period of the oscillation the London penetration depth of the MgB_2 film in *c*-axis is estimated to be 35 nm, consistent with theoretical prediction[25] and prior experimental measurements.[26] In contrast with the ideal Fraunhofer pattern, the minima of $I_c(B)$ do not reach zero and the oscillation amplitude does not decay monotonically at high field, indicating a nonuniform current distribution over the junction area. This may partially be due to that the Josephson penetration depth of this junction (20 μm) is comparable to the length of the junction (20 μm) (Ref. 1) and possible conductive shorts within the barrier. Figure 2(b) shows the $I-V$ curves of the junction under 17.1 GHz microwave radiations of various powers at 32 K. Shapiro steps were observed with step heights for different orders oscillating as the microwave power increases as shown in Fig. 2(c). The two experiments show unambiguously that the $MgB_2/MgO/MgB_2$ device is a Josephson junction.

The TEM image in Fig. 1(c) suggests an MgO barrier thickness of about 5 nm for the trilayer, larger than 1.5 nm determined by the deposition time. The discrepancy may be due to the rippling of the MgO layer through the thickness of the TEM sample or the oxide layer formed during the sample transfer in air and plasma oxidation during MgO sputtering.[27] Figure 3(a) shows a Rutherford back scattering (RBS) spectrum and simulation for an $MgB_2/MgO/MgB_2$ trilayer on SiC, the same as those used for the Josephson junctions. From the oxygen resonant scattering peak starting at channel number 200, the thickness of the MgO barrier is estimated to be 1.6 nm. Figure 3(b) is the $I-V$ curve of a junction showing steps due to the Fiske resonance modes (marked by arrows),[1] which arise from the coupling between the Josephson current and the electromagnetic mode inside the dielectric barrier layer. Using $\lambda_L=35$ nm and dielectric constant for MgO of 9.7,[28] the MgO layer thickness calculated from the steps is 1.2 nm, the same as determined from the deposition time. The two results are consistent with the thickness estimates from the deposition time, although errors can arise from oxygen vacancies in MgO for the RBS simulation and from the error in dielectric constant of MgO for the Fiske calculation.

Figure 4(a) shows an exponential dependence of J_c at 4.2 K on MgO barrier thickness, determined by the MgO deposition time. If we assume the simplest possible tunneling model for the Josephson current, $J_c=J_0\exp(-d/d_0)$, where $d_0=\hbar/(8mE_b)^{1/2}$ and E_b is the barrier height, we estimate E_b to be 0.8 eV, similar to that of MgO barriers in other tunnel junctions.[29] For an MgO layer thickness of 0.86 nm, J_c is 275 kA/cm^2 at 4.2 K, comparable to the highest J_c achieved in Nb junctions.[30] The $I_c(B)$ and $I-V$ curve of this junction at 4.2 K are shown in Fig. 4(b). From the high J_c value, one infers an ultimate speed limit for a MgB_2 RSFQ TFF frequency divider to be above 1 THz.[2]

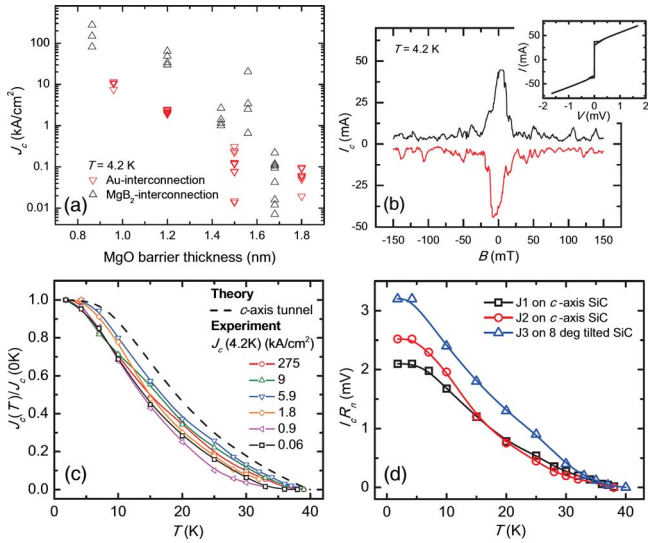

FIG. 4. (Color online) (a) J_c at 4.2 K for junctions of difference sizes on nine chips with Au or MgB_2 interconnection and MgO barrier thickness varying from 0.8 to 1.8 nm. (b) $I_c(B)$ and $I-V$ curve (inset) of a high J_c (275 kA/cm^2) junction (4×4 μm^2) at 4.2 K. (c) Normalized $J_c(T)$ of various junctions (solid lines) compared to the theoretical calculation for MgB_2 c-axis Josephson tunnel junction (dashed line). (d) $I_cR_n(T)$ of two c-axis (J1, J2) and one 8°-tilted (J3) junctions.

The behavior shown in Fig. 4(a) is different from that in $Nb/Al-AlO_x/Nb$ junctions, where the low-J_c junctions are superconductor-insulator-superconductor tunnel junctions and the high-J_c (>20 kA/cm^2) junctions are increasingly dominated by MAR. All the $MgB_2/MgO/MgB_2$ junctions we have studied show properties similar to those in high-J_c $Nb/Al-AlO_x/Nb$ junctions where MAR dominates. Whether some defect states or pinholes in the barriers are responsible for the MAR or not is a subject of ongoing investigation.

The temperature dependence of J_c for several $MgB_2/MgO/MgB_2$ junctions is shown in Fig. 4(c) along with the result of a two-band tunneling theory.[24] J_c remains nonzero up to 40 K. The faster decrease in J_c with increasing temperature than the theory is possibly due to weak link contributions.

In Fig. 4(d), I_cR_n versus temperature is shown for three junctions. J3 was made on a SiC substrate with 8° off cut to expose *ab* planes of the MgB_2 electrodes. The I_cR_n product at 4.2 K ranges from 2.1–3.1 mV, about half of the predicted value (4 and 6 mV for tunneling in *c* and *ab* directions, respectively).[24] J3 has the highest I_cR_n, possibly due to the σ band contribution.

For RSFQ circuits, superconducting interconnect is necessary.[1] Figure 4(a) shows that the J_c values for Au and MgB_2 interconnections are comparable, indicating that the $MgB_2/MgO/MgB_2$ junctions can survive the subsequent depositions of the insulator and MgB_2 layers. The on-chip J_c spread of ten $MgB_2/MgO/MgB_2$ junctions is ~10%, which needs to be reduced to 1%–2% for RSFQ circuits.

In summary, we have fabricated $MgB_2/MgO/MgB_2$ Josephson junctions with high J_c up to 275 kA/cm^2 at 4 K, which remains nonzero up to 40 K. Their properties resemble high-J_c $Nb/Al-AlO_x/Nb$ junctions. Improving the J_c uniformity, enhancing the I_cR_n product, and achieving nanometer-sized patterning for high-J_c junctions (~250 nm for I_c ~100 μA) are important next steps. Nevertheless, the results presented here should enable simple MgB_2 RSFQ circuits to demonstrate the ultrahigh speed of superconducting electronics at temperatures over 20 K.

We would like to thank John Rowell, Nate Newman, Ruggero Vaglio, Bob Burhman, and Bob Dynes for helpful discussions. The work is partially funded by ONR under Grant No. N00014-07-1-0079 (X.X.X.) and by DOE under Grant No. DE-FG02-08ER46531 (Q.L.). We acknowledge use of facilities at the PSU Site of the NSF NNIN.

[1] T. Van Duzer and C. W. Turner, *Principles of Superconductive Devices and Circuits*, 2nd ed. (Prentice Hall, New Jersey, 1998).
[2] NSA, Office of Corporate Assessments, Superconducting technology assessment 2005, available at http://www.nitrd.gov/pubs/nsa/sta.pdf.
[3] K. Likharev and V. Semenov, IEEE Trans. Appl. Supercond. **1**, 3 (1991).
[4] J. Rowell, Nature Mater. **1**, 5 (2002).
[5] H. J. M. ter Brake and G. F. M. Wiegerinck, Cryogenics **42**, 705 (2002).
[6] G. Carapella, N. Martucciello, G. Costabile, C. Ferdeghini, V. Ferrando, and G. Grassano, Appl. Phys. Lett. **80**, 2949 (2002).
[7] A. Saito, A. Kawakami, H. Shimakage, H. Terai, and Z. Wang, J. Appl. Phys. **92**, 7369 (2002).
[8] Y. Cui, K. Chen, Q. Li, X. X. Xi, and J. Rowell, Appl. Phys. Lett. **89**, 202513 (2006).
[9] G. Burnell, D. J. Kang, H. N. Lee, S. H. Moon, B. Oh, and M. G. Blamire, Appl. Phys. Lett. **79**, 3464 (2001).
[10] D. A. Kahler, J. Talvacchio, J. M. Murduck, A. Kirschenbaum, R. E. Brooks, S. B. Bu, J. Choi, D. M. Kim, and C. B. Eom, IEEE Trans. Appl. Supercond. **13**, 1063 (2003).
[11] K. Chen, Y. Cui, Q. Li, X. X. Xi, S. A. Cybart, R. C. Dynes, X. Weng, E. C. Dickey, and J. M. Redwing, Appl. Phys. Lett. **88**, 222511 (2006).
[12] D. Mijatovic, A. Brinkman, D. Veldhuis, H. Hilgenkamp, H. Rogalla, G. Rijnders, D. H. A. Blank, A. V. Pogrebnyakov, J. M. Redwing, S. Y. Xu, Q. Li, and X. X. Xi, Appl. Phys. Lett. **87**, 192505 (2005).
[13] S. Cybart, K. Chen, Y. Cui, Q. Li, X. X. Xi, and R. C. Dynes, Appl. Phys. Lett. **88**, 012509 (2006).
[14] H. Shimakage, K. Tsujimoto, Z. Wang, and M. Tonouchi, Appl. Phys. Lett. **86**, 072512 (2005).
[15] K. Ueda, S. Saito, K. Semba, T. Makimoto, and M. Naito, Appl. Phys. Lett. **86**, 172502 (2005).
[16] H. Shim, K. S. Yoon, J. S. Moodera, and J. P. Hong, Appl. Phys. Lett. **90**, 212509 (2007).
[17] L. A. Abelson and G. L. Kerber, Proc. IEEE **92**, 1517 (2004).
[18] W. Chen, A. V. Rylyakov, V. Patel, J. E. Lukens, and K. K. Likharev, IEEE Trans. Appl. Supercond. **9**, 3212 (1999).
[19] X. X. Xi, Rep. Prog. Phys. **71**, 116501 (2008).
[20] X. Zeng, A. V. Pogrebnyakov, A. Kotcharov, J. E. Jones, X. X. Xi, E. M. Lysczek, J. M. Redwing, S. Xu, Q. Li, J. Lettieri, D. G. Schlom, W. Tian, X. Pan, and Z. K. Liu, Nature Mater. **1**, 35 (2002).
[21] H. J. Choi, D. Roundy, H. Sun, M. L. Cohen, and S. G. Louie, Nature (London) **418**, 758 (2002).
[22] K. Chen, Y. Cui, Q. Li, C. G. Zhuang, Z. K. Liu, and X. X. Xi, Appl. Phys. Lett. **93**, 012502 (2008).
[23] A. W. Kleinsasser, R. E. Miller, W. H. Mallison, and G. B. Arnold, Phys. Rev. Lett. **72**, 1738 (1994).
[24] A. Brinkman, A. A. Golubov, H. Rogalla, O. V. Dolgov, J. Kortus, Y. Kong, O. Jepsen, and O. K. Andersen, Phys. Rev. B **65**, 180517(R) (2002).
[25] I. I. Mazin, O. K. Andersen, O. Jepsen, O. V. Dolgov, J. Kortus, A. A. Golubov, A. B. Kuz'menko, and D. van der Marel, Phys. Rev. Lett. **89**, 107002 (2002).
[26] B. B. Jin, T. Dahm, C. Iniotakis, A. I. Gubin, E. M. Choi, H. J. Kim, S. I. Lee, W. N. Kang, S. F. Wang, Y. L. Zhou, A. V. Pogrebnyakov, J. M. Redwing, X. X. Xi, and N. Klein, Supercond. Sci. Technol. **18**, L1 (2005).
[27] J. C. Read, P. G. Mather, and R. A. Buhrman, Appl. Phys. Lett. **90**, 132503 (2007).
[28] K. Senapati and Z. H. Barber, Appl. Phys. Lett. **94**, 173511 (2009).
[29] S. Yuasa, T. Nagahama, A. Fukushima, Y. Suzuki, and K. Ando, Nature Mater. **3**, 868 (2004).
[30] Z. Bao, M. Bhushan, S. Han, and J. E. Lukens, IEEE Trans. Appl. Supercond. **5**, 2731 (1995).